Key Points:

- Comparative study of seismic monitoring of rock in low (moisture) and intermediate (imbibition) saturation range
- Strong amplitude loss, very similar to moisture adsorption, but little and uncoupled velocity variations during spontaneous water imbibition
- Evidence for two competing effects of adsorption-induced softening and frequency-dependent stiffening during water imbibition

Correspondence to:

L. Pimienta,
lucas.pimienta@epfl.ch

Evolution in Seismic Properties During Low and Intermediate Water Saturation: Competing Mechanisms During Water Imbibition?

L. Pimienta[1] (iD), **C. David[2]** (iD), **J. Sarout[3]** (iD), **X. Perrot[4]** (iD), **J. Dautriat[3]** (iD), **and C. Barnes[2]** (iD)

[1]Laboratory of Experimental Rock Mechanics, Ecole Polytechnique Fédérale de Lausanne, Lausanne, Switzerland, [2]Laboratoire Géosciences et Environnement Cergy, Université de Cergy-Pontoise, Cergy-Pontoise, France, [3]CSIRO Energy, Perth, Western Australia, Australia, [4]Lab. de Métérologie Dynamique, Ecole Normale Supérieure, PSL University, Paris, France

Abstract Despite the efforts reported in the literature to explain contrasting experimental observations, the evolution of seismic attributes (velocity and attenuation) of rocks across the saturation range remains ill understood. In a comparative study, we monitored the evolution of ultrasonic *P* wave attributes in a porous sandstone subjected to two experiments of moisture adsorption and water spontaneous imbibition. Both experiments highlighted a significant (i.e., by 1 order of magnitude) and similar drop in *P* waves amplitudes, although the maximum saturations reached in each experiment is very different (i.e., about 2% vs. 70%). However, only moisture adsorption leads to a dramatic elastic softening (velocity reduction). This difference might be explained by the coupling between two competing physical mechanisms taking place during water imbibition, namely, elastic softening driven by water adsorption at the grain contact and elastic stiffening driven by full saturation of the grain contacts, at the ultrasonic frequency of the measurement.

1. Introduction

Information about the presence, nature, and movements of fluids in the crust is key to many applications in geosciences. Among the geophysical methods that allow probing remotely the rock formations at depth in a noninvasive manner (Knight et al., 2010; Knight & Dvorkin, 1992; Knight & Nolen-Hoeksema, 1990; Mavko et al., 2003), the velocity and attenuation of seismic waves were shown to be sensitive to the presence of saturating fluids (Johnston et al., 1979; Mavko et al., 1979, 2003; Murphy, 1985; Murphy et al., 1986; Prasad & Manghnani, 1997; Prasad & Meissner, 1992; Toksöz et al., 1976, 1979; Winkler & Murphy, 1995). At full water saturation, at the ultrasonic frequency of measurements, one main—elastic stiffening—phenomenon has been acknowledged and largely investigated over the last decades (Dvorkin et al., 1995; Guéguen & Palciauskas, 1994; Gurevich et al., 2010; Mavko et al., 2003; Mavko & Jizba, 1991; Müller et al., 2010; Murphy et al., 1986; O'Connell & Budiansky, 1974, 1977; Le Ravalec & Guéguen, 1996). In terms of elastic energy loss, wave attenuation peaks were shown to usually exist at frequencies below the ultrasonic frequency, corresponding to the characteristic time scale of fluid flow in the rock (Adelinet et al., 2011; Batzle et al., 2006; Fortin et al., 2014; Mavko & Jizba, 1991; Pimienta et al., 2016, 2017; Sarout, 2012; Winkler & Murphy, 1995). Although the elastic stiffening is expected to dominate in most rocks, another—elastic softening—effect has been observed in some rocks, of a decrease in elastic properties upon water saturation (Assefa et al., 1999, 2003; Baechle et al., 2008; Eberli et al., 2003). However, because elastic stiffening may always occur at or very near full saturation, it is difficult to isolate the softening effect at the ultrasonic frequency of measurement.

In order to investigate a possible cause of elastic softening unbiased by the stiffening effect, rocks were measured under very low degrees of saturation thanks to controlled moisture adsorption experiments (Pimienta, Fortin, & Gueguen, 2014; Yurikov et al., 2018). Although usually amounting to saturations below 3%, moisture adsorption was shown to lead to large decrease in elastic properties due to adsorption-induced mechanical softening at the grain contacts (Clark et al., 1980; Johnson et al., 1971; Murphy et al., 1986; Pimienta, Fortin, & Gueguen, 2014). However, although links to full saturation could be postulated from surface energy variations (Parks, 1984), no studies to date linked these two end-member scenarios.

Owing to the amount of mechanisms occurring depending on the saturating strategies, understanding quantitatively the dependence of seismic attributes to the saturation state of the rock remains a challenge (Chapman et al., 2016; David, Bertauld, et al., 2015; Lopes et al., 2014; Murphy et al., 1986; Papageorgiou & Chapman, 2015; Le Ravalec et al., 1996; Winkler & Murphy, 1995). One such strategy is to monitor the effects on *P* wave velocity and attenuation in spontaneous imbibition experiments (David, Bertauld, et al., 2015; Pons et al., 2011). Through an interaction between capillary, gravity, and wettability driving forces, fluids such as water can be spontaneously sucked in by a porous rock and migrate through its pore network, leading in some cases to large saturation at equilibrium (large times). Recent spontaneous imbibition experiments evidenced a strong reduction in ultrasonic wave amplitudes, with little changes in wave velocities (David, Barnes, et al., 2017; David, Sarout, et al., 2017). Those observations were attributed to diffusion of moisture migrating faster and ahead of the front of imbibing liquid water, thus leading to attenuation although not leading to strong elastic softening of grains contacts. However, during moisture adsorption experiments (no liquid water in contact with the rock), both attenuation and elastic softening were observed over the range of low saturations (i.e., below 3%) allowed by relative humidity (RH) variations (Bulau et al., 1984; Clark et al., 1980; Pimienta, Fortin, & Gueguen, 2014; Tittmann, Clark, & Spencer, 1980).

With the aim to understand the physics underlying the evolution in seismic properties across the saturation range, we carried a comparative study of seismic monitoring during moisture adsorption and spontaneous imbibition in two brother samples of loosely cemented Sherwood sandstone. From the measurements and physics underlying the evolution in properties during moisture adsorption, we infer a physical interpretation of two competing phenomena for the evolution in properties during water imbibition.

2. Materials and Methods

The rock used in this study is a Sherwood sandstone, a porous (i.e., 30% porosity) and poorly cemented Triassic sandstone originating from southwest coast of England, Ladram Bay Cliffs (Dautriat et al., 2016; David, Dautriat, et al., 2015; David, Barnes, et al., 2017; Nguyen et al., 2014). The mineral matrix consists of three main minerals: 43% quartz, 26% feldspars, and 17% clay minerals, with a mean grain size of 120 μm. This layered rock is slightly anisotropic (Nguyen et al., 2014), with (i) permeability in the range 200 to 350 mD and (ii) ultrasonic *P* wave velocity of dry samples between 1.4 and 1.8 km/s (Dautriat et al., 2016). At full water saturation, *P* wave velocity anisotropy was found to cancel, with an average *P* wave velocity of about 2.0 km/s (Dautriat et al., 2016).

Two horizontally layered twin samples were selected, one for the spontaneous water imbibition experiments (Figure 1a) and one for moisture adsorption experiments in controlled RH conditions (Figure 1b). Each sample is equipped with a pair of ultrasonic (0.5 MHz) *P* wave piezoelectric transducers glued in a diametrically opposed geometry onto the lateral surface of the sample. *P* wave velocities are measured at constant time intervals (i.e., every 10 s) during the spontaneous imbibition experiment (Figure 1a) and related to a measured RH value during the adsorption experiment (Figure 1b). Elastic wave data processing is the same for the two data sets (Figure 1c) and consists of automatically picking the minimum and maximum of the first wavelet and characterizing its relative variation in amplitude and traveltime (Pimienta, Fortin, & Gueguen, 2014). The experimental protocols are detailed in the supporting information.

3. Results

For the two experiments, the monitoring of water saturation from mass change of the sample could not be directly attained during the experiment. The maximum water saturation of the sample achieved was about 70% after the end of the spontaneous imbibition and about 2% after the moisture adsorption experiment. From the two experiments, the relative *P* wave velocity and amplitudes as a function of water imbibition (Figures 2a and 2c) and moisture adsorption (Figures 2b and 2d) are compared. Further discussion and measurements are provided in the supporting information.

3.1. Moisture Adsorption and Desorption

At the initiation of the experiment (Figures 2a and 2c, blue symbols), the sample was fully oven dry, and the measured *P* wave velocity (1.8 km/s) and amplitude were at their maximum value (Figure S1). As RH increases toward 80%, a small decrease in both amplitude and velocity was observed. Once RH exceeds
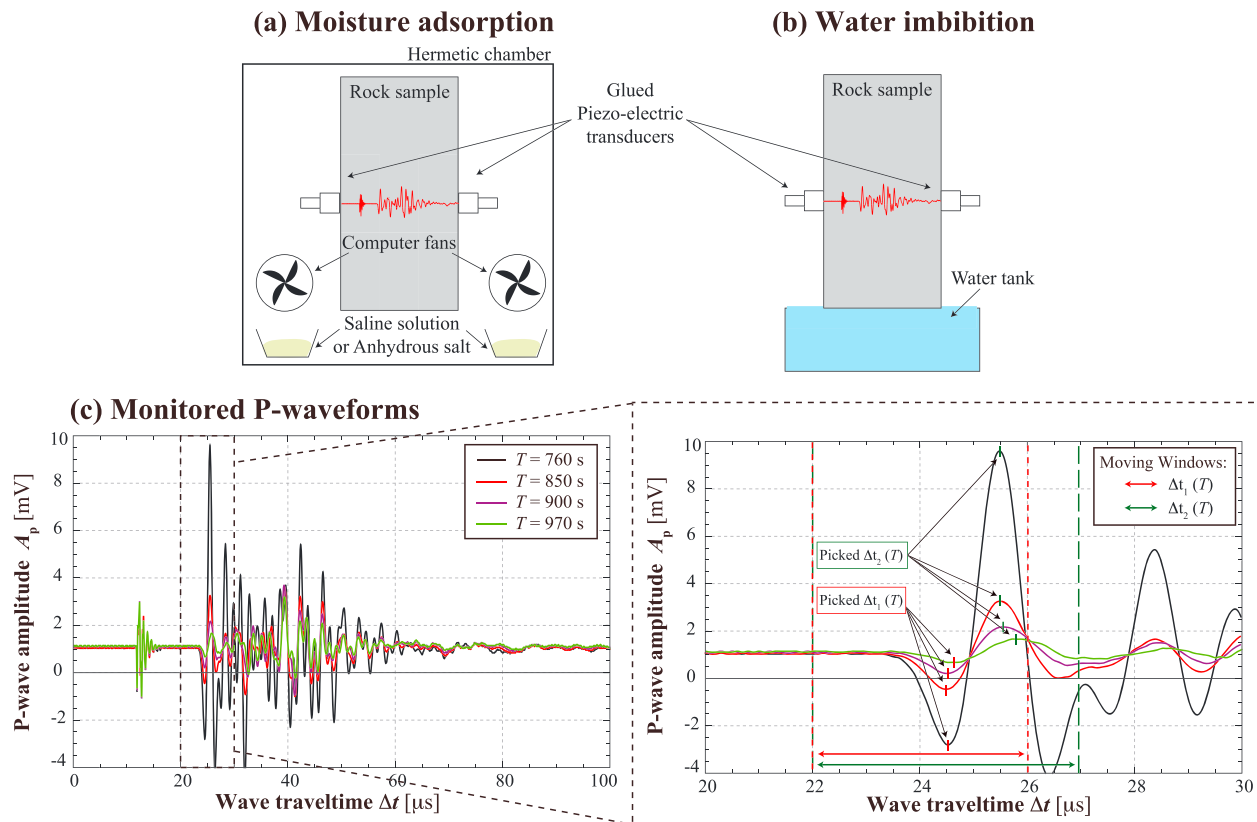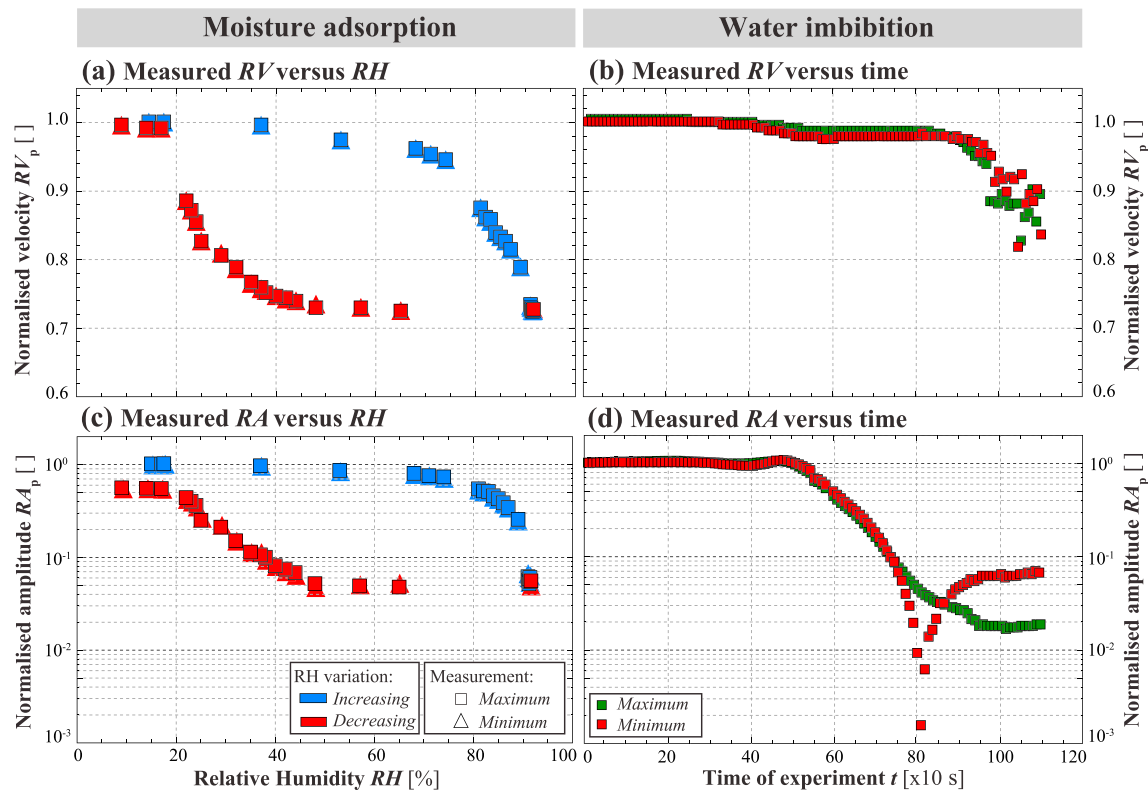
Figure 1. Principle of the experimental procedures for *P* wave ultrasonic velocities monitoring during (a) controlled moisture adsorption and (b) spontaneous water imbibition in the rock sample. For controlled moisture adsorption, computer fans are used for fast equilibration of the air relative humidity during the experiment, so that the read relative humidity value equals that inside the porosity. (c) The monitored waveforms are processed with the same automatic procedure to get the relative variations in amplitudes and traveltimes.

this value, an exponential decrease was observed in both properties. Overall, a decrease of about 30% and 80% was recorded for velocities and amplitudes, respectively, over the RH range (i.e., from 8% to about 92% RH).

After equilibration at the maximum RH of about 92%, the saline solution was replaced by an anhydrous salt in the controlled atmosphere chamber to induce the progressive drying of the moist sample (Figures 2a and 2c, red symbols). At that point, RH remained at very high values (i.e., about 92%) over a relatively long time, and *P* wave velocities and amplitudes remained at their lowest. Then, RH slowly decreased as the anhydrous salt absorbed progressively the moist evaporating from the sample. Above 50% RH, *P* wave velocities and amplitudes remained low so that a strong hysteresis is observed. With a further decrease of RH from 40% to 20%, both amplitudes and velocities showed a dramatic increase as adsorbed water was forcibly removed from the sample internal surface. As RH further decreased down to 10%, no further increase was observed, while the *P* wave amplitude and velocity only nearly reached their initial values (oven-dry state prior to the experiment). After the experiment, the sample was again fully oven dried and the sample fully recovered its initial values of velocity and amplitude, indicating that this phenomenon is reversible.

3.2. Spontaneous Imbibition

At the early stages of spontaneous water imbibition experiment (Figures 2b and 2d), *P* wave velocity and amplitude remained constant. The *P* wave velocity value of about 1.75 km/s is consistent with that from the moisture adsorption study, with a room RH of about 50–60%. Once the water-front arrived into the probed Fresnel zone (Figure S2), *P* wave velocities only slightly decreased and amplitudes showed a small decrease then increase. Beyond this point, amplitudes strongly decreased and stabilized to a minimum, of about 1% of its initial value. The decrease in amplitude was much slower than the inferred saturations in

AGU
100
ADVANCING EARTH
AND SPACE SCIENCE

Geophysical Research Letters

10.1029/2019GL082419

Figure 2. Relative variations of (a, b) *P* wave velocity and (c, d) *P* wave amplitude on the two brother samples of Sherwood sandstone, during the two experiments of (a, c) moisture adsorption and (b, d) water imbibition.

the probed zone (Figure S1), which originate from the difference in volumes probed with both techniques. *P* wave velocities were almost constant over the whole experiment, although showing a slight progressive decrease before times of 800 s.

At times larger than about 800 s, velocities however decreased to about 90% of its initial value. Interestingly, this decrease correlates to a decrease in the inferred saturation in the zone representative of the Fresnel zone. Note that, because the amplitude decreased by 2 orders of magnitude during the experiment, the accuracy of the traveltime picking decreased. Hence, no much implication will be given for the decreases observed beyond times of 800 s.

4. Interpretations

The time-lapse moisture adsorption data suggest that both elastic softening and energy loss occur, and the phenomenon appears fully reversible (Figures 2a and 2c), that is, the elastic properties of the initial rock are recovered after drying the sample. However, the time-lapse imbibition data indicate that essentially only energy loss occurs (Figure 3a and 3c) and, although a slight velocity softening is observed, it remains marginal compared to the amplitude loss. In order to gain a better understanding on the underlying physics, we compare the two data sets based on the micromechanics of adsorption at grain contacts.

4.1. Elastic Softening by Moisture Adsorption

Physical adsorption of water molecules in the pore network is a good candidate to explain the reversible elastic softening observed during the moisture adsorption experiment (Johnson et al., 1971; Murphy et al., 1986; Pimienta, Fortin, & Gueguen, 2014). Earlier works showed that strong softening could occur upon moisture adsorption in sandstones (Clark et al., 1980) and that it was not an effect of the clay minerals as particularly strong effects could be obtained in quartz-pure sandstones (Pimienta, Fortin, & Gueguen, 2014). As further reported in the literature, elastic softening was found to correlate with the amplitude loss and thus *P* wave
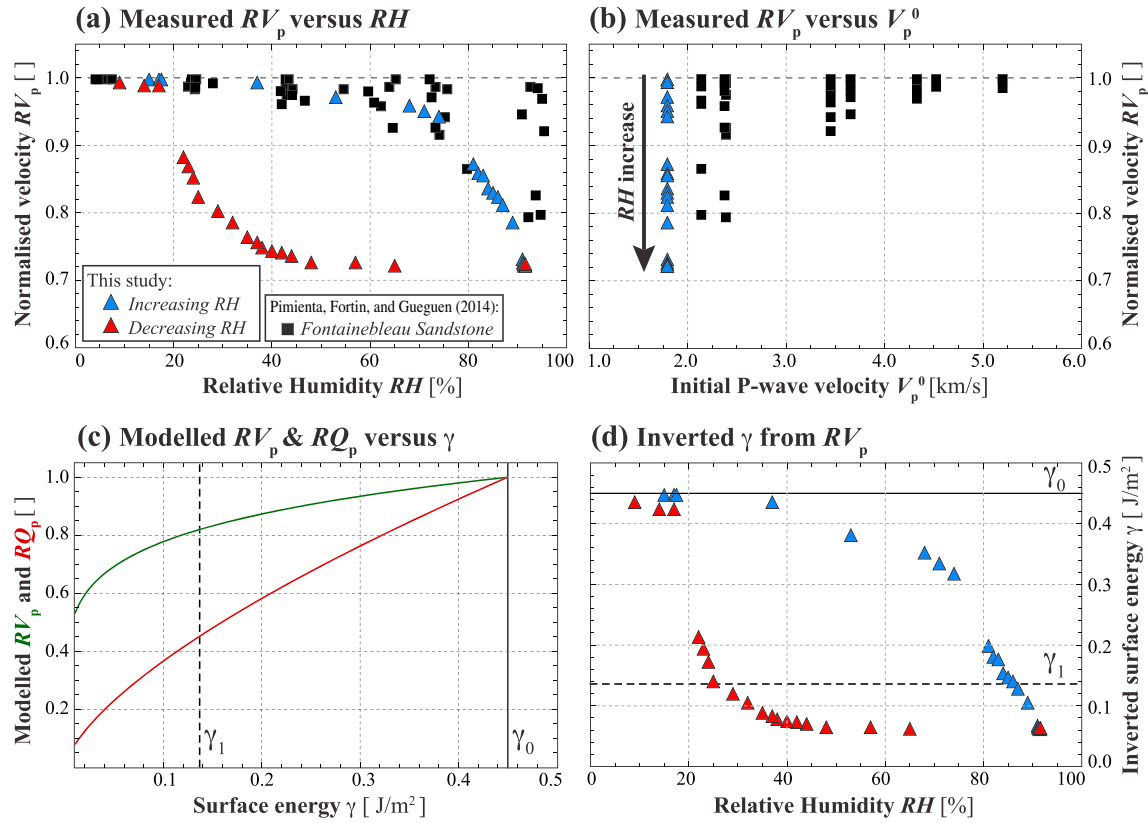
Figure 3. Comparison between this study and one published (Pimienta, Fortin, & Gueguen, 2014) on the effects of moisture adsorption on *P* wave velocities. The relative V_p variations (i.e., RV_p) are plotted as a function (a) of RH and (b) of the samples initial dry *P* wave velocities. Fontainebleau sandstone samples reported (Pimienta, Fortin, & Gueguen, 2014) span a range in porosity from about 3% to about 18%. (c) Comparison between predicted elastic (RV_p, equation (2)) softening and energy dissipation (RQ_p, equation (4)) from surface energy variations, and (d) inferred surface energy variation with RH from least squares inversion between model (equation (2)) and measurement. Quartz surface energy under dry (γ_0) and water-saturated (γ_1) conditions are reported for comparison.

attenuation, which is consistent with what is observed here (Clark et al., 1980; Pimienta, Fortin, & Gueguen, 2014; Tittmann, Clark, Richardson, et al., 1980; Yurikov et al., 2018). Existing dissipative effects that could be considered are the frequency-dependent squirt flow (e.g., Gurevich et al., 2010) or frequency-independent dissipation at grain contact (e.g. Prasad & Meissner, 1992). Noting further that existing measurements reported the same variations in both velocity and amplitude, measured at very different frequency of 0.1–1 kHz (Clark et al., 1980; Tittmann, 1977, 1978) and 0.5–1 MHz (Pimienta, Fortin, & Gueguen, 2014), we investigate here the frequency-independent effects: softening and dissipation at grain contact.

Comparing the present measurements with the ones reported using a similar experimental setup (Pimienta, Fortin, & Gueguen, 2014), very similar elastic softening is observed as RH increases (Figure 3a), that is, down by 20–30%. Although mineralogy is more complex in the Sherwood than in the quartz-pure Fontainebleau sandstone, other differences exist that could explain the larger variations. The Sherwood sandstone has a porosity of 30% and a smaller mean grain size *d* (i.e., $d \sim 100\,\mu m$) compared to the Fontainebleau sandstone (i.e., $d \sim 200\,\mu m$). Comparing the variations to the *P* wave velocity of dry samples (Figure 3b), a good correlation exists between the sample stiffness (i.e., *P* wave velocity) and the softening effect from adsorption. This could originate from the difference in rocks grain size, as postulated in JKR's theory (Johnson et al., 1971). According to this theory, surface forces affect Hertzian contact radius a_0, so that the area of contact a_1 between two grains is (Johnson et al., 1971)

$$a_1{}^3 = a_0{}^3 + \frac{3(1-\nu_m)r}{8G_m}\left[6\gamma\pi r + \sqrt{12\gamma\pi rF + (6\gamma\pi r)^2}\right], \tag{1}$$

where G_m and ν_m are the minerals/grains elastic constants and *r* is the grain radius. The Hertzian contact

area a_0 is a constant in case of constant external force F applied to a rock sample, but a_1 varies with the moisture adsorption affecting the surface energy γ at the contact between two grains. Because both normal and tangential stiffness are a direct function of the area of contact (Mindlin, 1949), they intrinsically depend on γ (Johnson et al., 1971). It follows that the effective elastic moduli of the granular assemblage (the rock) are also a direct function of γ (Murphy et al., 1984; Pimienta, Fortin, & Gueguen, 2014). Assuming the rock to be weakly cemented, monitoring the relative variations in P wave velocity (i.e., hence P wave modulus $M_1 = \rho V_p^2$) during moisture adsorption allows to directly infer the change in surface area at the grain contact (Pimienta, Fortin, & Gueguen, 2014):

$$\frac{M_1}{M_{1_0}} = \frac{a_1}{a_{1_0}} = f(G_m, \nu_m, r, F, \gamma) = f(\gamma). \tag{2}$$

Hence, the change in V_p is strictly equal to the change in contact radius from surface force variations. As it was not investigated before, it is of further interest to question whether the waves amplitude—directly linked to the waves attenuations—might also be affected by adsorption of water molecules. According to Prasad and Meissner (1992; i.e., equation 14), based on the Hertzian contact theory (Digby, 1981; Mindlin, 1949), energy dissipation from frictional losses may be calculated from the shear strength at the grain contact in a volume containing a known amount of grains and grain contacts. The equation (Prasad & Meissner, 1992) outlines the fact that Q_s^{-1} is a function of a_1 such that

$$Q_s^{-1} = Cst \frac{1}{a} \left[\frac{3b}{(2-\nu_m)} + \frac{a}{(1-\nu_m)} \right]^3 \sim Cst_1 \, a^2, \tag{3}$$

where Cst is a combination of various parameters (see equation 14 of Prasad & Meissner, 1992, for details), all constants except for a in the present study. Because the rock is loosely cemented, it can safely be assumed that the bounding radius is $b \ll a$, so that Q_s^{-1} is proportional to a^2 (equation (3)). Based on the observation that P and S wave velocities and amplitude variations were similarly affected by moisture adsorption (Pimienta, Fortin, & Gueguen, 2014), one might thus assume that Q_p^{-1} is also a function of a_1^2, that is,

$$\frac{Q_1^{-1}}{Q_{1_0}^{-1}} \sim \left(\frac{a_1}{a_{1_0}} \right)^2 = g(G_m, \nu_m, r, F, \gamma) = g(\gamma). \tag{4}$$

As surface energy γ decreases at the grain contact, both elastic softening and wave energy loss will thus occur, but dissipation might be approximately twice that of the elastic softening from moisture adsorption (Figure 3c). Because the measured amplitude ratio (Figures 2b and 2d) is proportional to the dissipation coefficient, the stronger decrease in amplitudes as compared to velocities is consistent with equation (4). We focus our attention here on the comparison between measured and modeled elastic softening. From a least squares minimization of the difference between measured and modeled P wave velocity (equation (1)), the mean surface energy γ is inverted as a function of RH (Figure 3d). The results capture well—both qualitatively and quantitatively—the reported variations in γ as a function of RH expected for a clean quartz surface (Parks, 1984).

4.2. Water Imbibition: Competing Mechanisms?

One notes in Figure 2 that (i) very similar variations in P wave amplitudes are observed in the moisture adsorption and water imbibition experiments (Figure 2c and 2d) and (ii) correlated variations are observed between P wave velocities (Figure 2a) and amplitudes (Figure 2c) during moisture adsorption, which is consistent with model predictions (Figure 3c).

The first observation suggests that the same physical mechanism causes the amplitude decrease (wave energy loss) in both types of experiments, that is, physical adsorption of water molecules at grain contacts (Figure 3c). Assuming that this interpretation is valid, the second observation suggests that the difference in P wave velocity changes observed in the two types of experiments could be due to an additional physical mechanism operative during water imbibition and not during moisture adsorption. This additional mechanism should counterbalance, at least partially, the adsorption-induced velocity softening but should not affect the waves amplitude. Such a velocity stiffening mechanism has been reported in the literature for porous and cracked rocks: elastic stiffening at the ultrasonic frequency of measurement (Batzle et al., 2006;
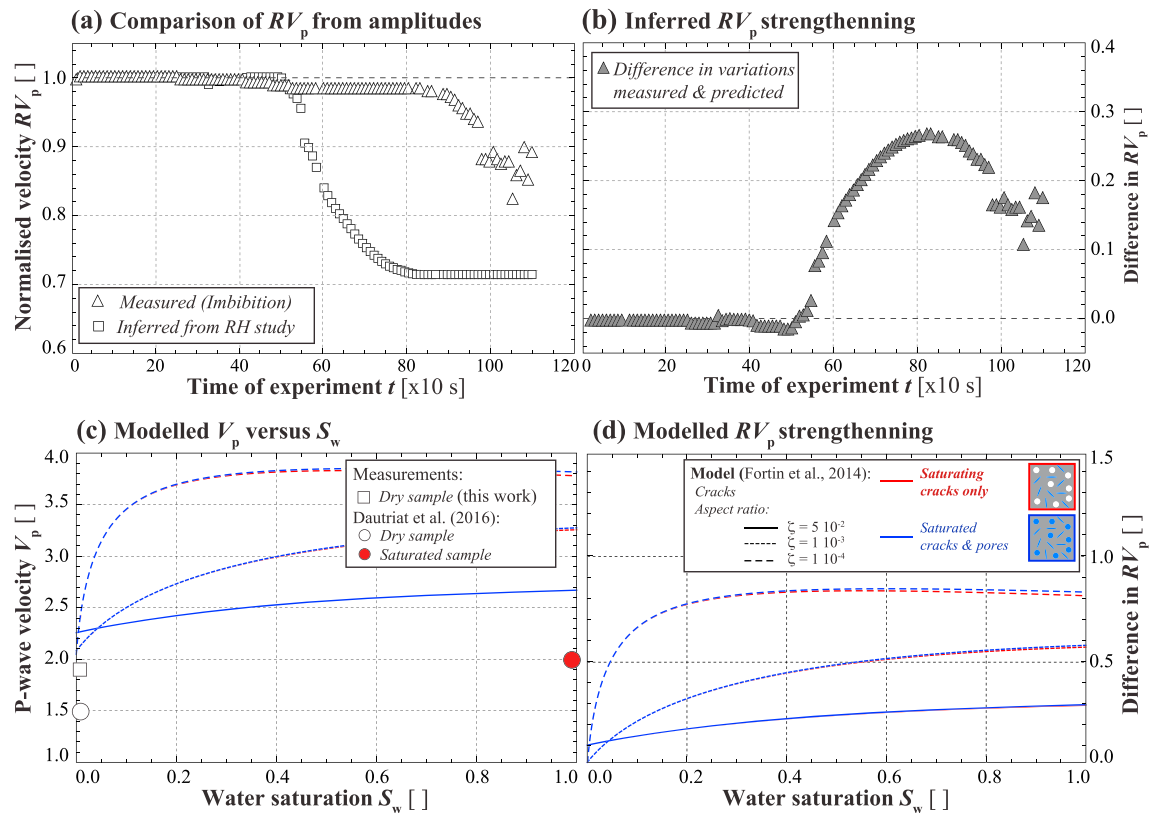
Figure 4. (a) Comparison between imbibition and *RH*-inferred velocity variation data from using a least squares minimization for the *RH* value corresponding to the measured amplitude variation. (b) Inferred difference in *P* wave velocity variation between the two studies, showing the uncoupling from adsorption-induced softening effect and a stiffening during water spontaneous imbibition. Prediction of the effect of partial saturation S_w in a porous and microcracked (or open grain contacts) medium (Fortin et al., 2007), with the realistic extreme range of crack aspect ratio values from 10^{-4} to $5*10^{-3}$, accounting separately for saturation of cracks only (i.e., red curves) or of both cracks and pores (i.e., blue curves) for (c) *P* wave velocity and (d) *P* wave velocity variation (i.e., difference RV_p).

Fortin et al., 2014; Müller et al., 2010). Studies further showed that—in most sandstones—no attenuation peak should be measured at ultrasonic frequencies (Pimienta et al., 2015a, 2015b, 2017; Subramaniyan et al., 2015). Hence, consistent with the conditions for the sought mechanism, waves amplitudes should not be affected at the ultrasonic frequency of measurement.

To investigate further this effect, the amplitude variations with RH during the adsorption experiment are fitted with a polynomial function (i.e., $A_p = f(\text{RH})$). From a least squares minimization between the function and the measurement, a fictive RH value corresponding to each amplitude variation during the imbibition study is inverted and then used as an input to predict the variation in *P* wave velocity (Figure 4a, gray squares) expected—from moisture adsorption—during imbibition, if only adsorption-induced softening was to occur. As inferred from the amplitude variations, the total softening from adsorption of water molecules is expected to occur fast, a time at which no variation was yet recorded on the measured *P* wave velocity (Figure 4a, black squares). Moreover, whichever the time, much larger decrease in velocity is expected than that actually measured.

Let us assume that in both moisture adsorption and water imbibition experiments the wave energy loss (amplitude reduction) is exclusively due to the adsorption of water molecules at grain contacts. The lack of significant velocity softening (reduction) observed in the water imbibition experiment is then attributed to a competing velocity stiffening mechanism, which counterbalances the velocity softening expected form water adsorption.

Plotting the difference between the relative velocity variations (i.e., RV_p) observed in the two types of experiments (Figure 4b) highlights a progressive increase in V_p as imbibition proceeds, up to a point where V_p decreases again. The increase with time could relate to an increasing amount of water-saturated grain

contacts. Provided that saturation occurs during this time frame, such an interpretation relies on two underlying assumptions, that is, that (1) the grain contacts—rather than the bulk porosity—will be saturated first during imbibition, and (2) the elastic stiffening associated with saturating grain contacts is sufficiently large to be measurable (and compete with the adsorption-driven softening) at the macroscopic scale by the time-lapse ultrasonic monitoring of the rock.

Similar to the capillary rise in a granular medium, because open grain contacts have much smaller equivalent pore radius (aperture or aspect ratio) when compared to spherical (equant) pores, capillary rise is likely to be driven predominantly by preferential saturation of the grain contacts. To assess the validity of assumption (2), we use Kachanov's effective medium approach (Kachanov, 1993; Guéguen & Kachanov, 2011; Fortin et al., 2007; Pimienta, Sarout, et al., 2014) and apply it to a porous sandstone with microcracks simulating grain contacts. This allows us to discriminate the impact on P wave velocity of the preferential saturation of the equant or crack-like pores (grain contacts). To this end, we use a micromechanical model developed by Fortin et al. (2007) specifically for porous and microcracked sandstones. The advantage of this model is that the impact on P wave velocity of the equant and crack-like pores are explicitly (analytically) accounted for by superposition, neglecting the stress and fluid interactions between them.

Using this model, calibrated in terms of crack density to fit with the values of V_p measured in the dry Sherwood sandstone, it is possible to predict the effect of saturating either all the porosity (Figure 4c, blue curves) or only the network of grain contacts (Figure 4c, red curves). The modeling results show that a relatively small effect on P wave velocity is expected from varying the saturation of the equant pores alone. The dominant effect actually originates from the saturation of crack-like pores/grain contacts (Figure 4c). The prediction, attempted for an expected range of realistic crack aspect ratio values, further shows that large increases might be expected even at low saturation stages even in the case where only open grain contacts are saturated (Figure 4c, red curves). Inferring the expected relative variations (Figure 4d), much larger than that inferred (Figure 4b) increase, could be predicted depending on the aspect ratio value, even at low saturation stages.

As for softening effects, this interpretation assumes that the same dissipation mechanism occurs at both very low (i.e., RH) and intermediate saturations (i.e., imbibition) and that this mechanism is of dissipation at grain contact (Prasad & Meissner, 1992). The frequency-dependent squirt flow could also occur at elevated saturations and add up to the frictional dissipation during the RH study. While it could explain the further decrease in amplitudes, it would however imply for very large aspect ratio (i.e., 1–5 10^{-2}) of the open grain contacts. From the computerized tomography monitoring, local water saturation was observed and reached its maximum at the onset of most variations in acoustic properties (Figure S2). Accounting for the restricted volume of monitoring, that is, about two fifths of the sample diameter, it is consistent with measured amplitude variations.

5. Conclusions

The P wave velocity and amplitude of two brother samples of sandstone were measured in two joint experiments, as a function of moisture adsorption and spontaneous imbibition. From the moisture adsorption study, large decrease in both P wave velocity and amplitude were observed as RH increased. This effect occurs from adsorption of water molecules at the contact between two grains that decrease the attractive force resulting from surface energies, leading to elastic softening. From spontaneous imbibition, a very large decrease in P wave amplitudes is observed, yet P wave velocities remain almost constant over all the recorded time. Assuming that the decrease in amplitude originates from the same physics as moisture adsorption, this observation is interpreted as the combination of two opposite effects: (i) water softening from moisture adsorption, affecting equally elasticity and attenuation, and (ii) elastic stiffening of water when measured at ultrasonic frequencies, consistently not affecting the amplitudes.

References

Adelinet, M., Fortin, J., & Guéguen, Y. (2011). Dispersion of elastic moduli in a porous-cracked rock: Theoretical predictions for squirt-flow. *Tectonophysics*, *503*(1–2), 173–181. https://doi.org/10.1016/j.tecto.2010.10.012

Assefa, S., McCann, C., & Sothcott, J. (1999). Attenuation of P- and S-waves in limestones. *Geophysical Prospecting*, *47*(3), 359–392. https://doi.org/10.1046/j.1365-2478.1999.00136.x

Assefa, S., McCann, C., & Sothcott, J. (2003). Velocities of compressional and shear waves in limestones. *Geophysical Prospecting*, *51*(1), 1–13. https://doi.org/10.1046/j.1365-2478.2003.00349.x

Baechle, G. T., Colpaert, A., Eberli, G. P., & Weger, R. J. (2008). Effects of microporosity on sonic velocity in carbonate rocks. *The Leading Edge*, *27*(8), 1012–1018. https://doi.org/10.1190/1.2967554

Batzle, M. L., Han, D.-H., & Hofmann, R. (2006). Fluid mobility and frequency-dependent seismic velocity: Direct measurements. *Geophysics*, *71*(1), N1–N9. https://doi.org/10.1190/1.2159053

Bulau, J. R., Tittmann, B. R., Abdel-Gawad, M., & Salvado, C. (1984). The role of aqueous fluids in the internal friction of rock. *Journal of Geophysical Research*, *89*(B6), 4207–4212. https://doi.org/10.1029/JB089iB06p04207

Chapman, S., Tisato, N., Quintal, B., & Holliger, K. (2016). Seismic attenuation in partially saturated Berea sandstone submitted to a range of confining pressures. *Journal of Geophysical Research: Solid Earth*, *121*, 1664–1676. https://doi.org/10.1002/2015JB012575

Clark, V. a., Tittmann, B. R., & Spencer, T. W. (1980). Effect of volatiles on attenuation (Q^{-1}) and velocity in sedimentary rocks. *Journal of Geophysical Research*, *85*(B10), 5190–5198. https://doi.org/10.1029/JB085iB10p05190

Dautriat, J., Sarout, J., David, C., Bertauld, D., & Macault, R. (2016). Remote monitoring of the mechanical instability induced by fluid substitution and water weakening in the laboratory. *Physics of the Earth and Planetary Interiors*, *261*, 69–87. https://doi.org/10.1016/j.pepi.2016.06.011

David, C., Barnes, C., Desrues, M., Pimienta, L., Sarout, J., & Dautriat, J. (2017). Ultrasonic monitoring of spontaneous imbibition experiments: Acoustic signature of fluid migration. *Journal of Geophysical Research: Solid Earth*, *122*, 4931–4947. https://doi.org/10.1002/2016JB013804

David, C., Bertauld, D., Dautriat, J., Sarout, J., Menéndez, B., & Nabawy, B. (2015). Detection of moving capillary front in porous rocks using X-ray and ultrasonic methods. *Frontiers in Physics*, *3*, 53. https://doi.org/10.3389/fphy.2015.00053

David, C., Dautriat, J., Sarout, J., Delle Piane, C., Menéndez, B., Macault, R., & Bertauld, D. (2015). Mechanical instability induced by water weakening in laboratory fluid injection tests. *Journal of Geophysical Research: Solid Earth*, *120*, 4171–4188. https://doi.org/10.1002/2015JB011894

David, C., Sarout, J., Dautriat, J., Pimienta, L., Michée, M., Desrues, M., & Barnes, C. (2017). Ultrasonic monitoring of spontaneous imbibition experiments: Precursory moisture diffusion effects ahead of water front. *Journal of Geophysical Research: Solid Earth*, *122*, 4948–4962. https://doi.org/10.1002/2017JB014193

Digby, P. J. (1981). The effective elastic moduli of porous granular rocks. *Journal of Applied Mechanics*, *48*(4), 803. https://doi.org/10.1115/1.3157738

Dvorkin, J., Mavko, G., & Nur, A. (1995). Squirt flow in fully saturated rocks. *Geophysics*, *60*(1), 97–107. https://doi.org/10.1190/1.1443767

Eberli, G. P., Baechle, G. T., Anselmetti, F. S., & Incze, M. L. (2003). Factors controlling elastic properties in carbonate sediments and rocks. *The Leading Edge*, *22*(7), 654–660. https://doi.org/10.1190/1.1599691

Fortin, J., Guéguen, Y., & Schubnel, A. (2007). Effects of pore collapse and grain crushing on ultrasonic velocities and V_p/V_s. *Journal of Geophysical Research*, *112*, B08207. https://doi.org/10.1029/2005JB004005

Fortin, J., Pimienta, L., Guéguen, Y., Schubnel, A., David, E. C., & Adelinet, M. (2014). Experimental results on the combined effects of frequency and pressure on the dispersion of elastic waves in porous rocks. *The Leading Edge*, *33*(6), 648–654. https://doi.org/10.1190/tle33060648.1

Guéguen, Y., & Kachanov, M. (2011). Effective elastic properties of cracked rocks: An overview. In *Mechanics of crustal rocks*, *CISM Courses and Lectures* (Vol. 533, pp. 73–125). Vienna: Springer.

Guéguen, Y., & Palciauskas, V. (1994). *Introduction to the physics of rocks*. Princeton, NJ: Princeton University Press.

Gurevich, B., Makarynska, D., de Paula, O. B., & Pervukhina, M. (2010). A simple model for squirt-flow dispersion and attenuation in fluid-saturated granular rocks. *Geophysics*, *75*(6), N109–N120. https://doi.org/10.1190/1.3509782

Johnson, K. L., Kendall, K., & Roberts, A. D. (1971). Surface energy and the contact of elastic solids. *Proceedings of the Royal Society of London. A. Mathematical and Physical Sciences*, *324*(1558), 301–313. https://doi.org/10.1098/rspa.1971.0141

Johnston, D. H., Toksöz, M. N., & Timur, A. (1979). Attenuation of seismic waves in dry and saturated rocks: II. Mechanisms. *Geophysics*, *44*(4), 691–711. https://doi.org/10.1190/1.1440970

Kachanov, M. (1993). Elastic solids with many cracks and related problems. *Advances in Applied Mechanics*, *30*, 259–445. https://doi.org/10.1016/S0065-2156(08)70176-5

Knight, R. J., & Dvorkin, J. (1992). Seismic and electrical properties of sandstones at low saturations. *Journal of Geophysical Research*, *97*(B12), 17,417–17,425. https://doi.org/10.1029/92JB01794

Knight, R. J., & Nolen-Hoeksema, R. (1990). A laboratory study of the dependence of elastic wave velocities on pore scale fluid distribution. *Geophysical Research Letters*, *17*(10), 1529–1532. https://doi.org/10.1029/GL017i010p01529

Knight, R. J., Pyrak-Nolte, L. J., Slater, L., Atekwana, E., Endres, A., Geller, J., et al. (2010). Geophysics at the interface: Response of geophysical properties to solid-fluid, fluid-fluid, and solid-solid interfaces. *Reviews of Geophysics*, *48*, RG4002. https://doi.org/10.1029/2007RG000242

Le Ravalec, M., & Guéguen, Y. (1996). High-and low-frequency elastic moduli for a saturated porous/cracked rock-differential self-consistent and poroelastic theories. *Geophysics*, *61*(4), 1080–1094. https://doi.org/10.1190/1.1444029

Le Ravalec, M., Guéguen, Y., & Chelidze, T. (1996). Elastic wave velocities in partially saturated rocks: Saturation hysteresis. *Journal of Geophysical Research*, *101*(B1), 837–844. https://doi.org/10.1029/95JB02879

Lopes, S., Lebedev, M., Müller, T. M., Clennell, M. B., & Gurevich, B. (2014). Forced imbibition into a limestone: Measuring P-wave velocity and water saturation dependence on injection rate. *Geophysical Prospecting*, *62*(5), 1126–1142. https://doi.org/10.1111/1365-2478.12111

Mavko, G., & Jizba, D. (1991). Estimating grain-scale fluid effects on velocity dispersion in rocks. *Geophysics*, *56*(12), 1940–1949. https://doi.org/10.1190/1.1443005

Mavko, G., Kjartansson, E., & Winkler, K. (1979). Seismic wave attenuation in rocks. *Reviews of Geophysics*, *17*(6), 1155–1164. https://doi.org/10.1029/RG017i006p01155

Mavko, G., Mukerji, T., & Dvorkin, J. (2003). *The rock physics handbook: Tools for seismic analysis of porous media*. Cambridge, UK: Cambridge University Press.

Mindlin, R. D. (1949). Compliance of elastic bodies in contact: Transactions of American Society of Mechanical Engineers. *Journal of Applied Mechanics*, *16*, 259–268.

Müller, T. M., Gurevich, B., & Lebedev, M. (2010). Seismic wave attenuation and dispersion resulting from wave-induced flow in porous rocks—A review. *Geophysics*, *75*(5), 75A147–75A164. https://doi.org/10.1190/1.3463417

Murphy, W. F. III (1985). Sonic and ultrasonic velocities: Theory versus experiment. *Geophysical Research Letters*, *12*(2), 85–88. https://doi.org/10.1029/GL012i002p00085

Murphy, W. F. III, Winkler, K. W., & Kleinberg, R. L. (1984). Frame modulus reduction in sedimentary rocks: The effect of adsorption on grain contacts. *Geophysical Research Letters*, *11*(9), 805–808. https://doi.org/10.1029/GL011i009p00805

Murphy, W. F. III, Winkler, K. W., & Kleinberg, R. L. (1986). Acoustic relaxation in sedimentary rocks: Dependence on grain contacts and fluid saturation. *Geophysics*, *51*(3), 757–766. https://doi.org/10.1190/1.1442128

Nguyen, V. H., Gland, N., Dautriat, J., David, C., Wassermann, J., & Guélard, J. (2014). Compaction, permeability evolution and stress path effects in unconsolidated sand and weakly consolidated sandstone. *International Journal of Rock Mechanics and Mining Sciences*, *67*, 226–239. https://doi.org/10.1016/j.ijrmms.2013.07.001

O'Connell, R. J., & Budiansky, B. (1974). Seismic velocities in dry and saturated cracked solids. *Journal of Geophysical Research*, *79*(35), 5412–5426. https://doi.org/10.1029/JB079i035p05412

O'Connell, R. J., & Budiansky, B. (1977). Viscoelastic properties of fluid-saturated cracked solids. *Journal of Geophysical Research*, *82*(36), 5719–5735. https://doi.org/10.1029/JB082i036p05719

Papageorgiou, G., & Chapman, M. (2015). Multifluid squirt flow and hysteresis effects on the bulk modulus-water saturation relationship. *Geophysical Journal International*, *203*(2), 814–817. https://doi.org/10.1093/gji/ggv333

Parks, G. A. (1984). Surface and interfacial free energies of quartz. *Journal of Geophysical Research*, *89*(B6), 3997–4008. https://doi.org/10.1029/JB089iB06p03997

Pimienta, L., Borgomano, J. V. M., Fortin, J., & Guéguen, Y. (2017). Elastic dispersion and attenuation in fully saturated sandstones: Role of mineral content, porosity and pressures. *Journal of Geophysical Research: Solid Earth*, *122*, 9950–9965. https://doi.org/10.1002/2017JB014645

Pimienta, L., Fortin, J., Borgomano, J. V. M., & Guéguen, Y. (2016). Dispersions and attenuations in a fully saturated sandstone: Experimental evidence for fluid flows at different scales. *The Leading Edge*, *35*(6), 495–501. https://doi.org/10.1190/tle35060495.1

Pimienta, L., Fortin, J., & Gueguen, Y. (2014). Investigation of elastic weakening in limestone and sandstone samples from moisture adsorption. *Geophysical Journal International*, *199*(1), 335–347. https://doi.org/10.1093/gji/ggu257

Pimienta, L., Fortin, J., & Guéguen, Y. (2015a). Bulk modulus dispersion and attenuation in sandstones. *Geophysics*, *80*(2), D111–D127. https://doi.org/10.1190/geo2014-0335.1

Pimienta, L., Fortin, J., & Guéguen, Y. (2015b). Experimental study of Young's modulus dispersion and attenuation in fully saturated sandstones. *Geophysics*, *80*(5), L57–L72. https://doi.org/10.1190/geo2014-0532.1

Pimienta, L., Sarout, J., Esteban, L., & Piane, C. D. (2014). Prediction of rocks thermal conductivity from elastic wave velocities, mineralogy and microstructure. *Geophysical Journal International*, *197*(2), 860–874. https://doi.org/10.1093/gji/ggu034

Pons, A., David, C., Fortin, J., Stanchits, S., Menéndez, B., & Mengus, J. M. (2011). X-ray imaging of water motion during capillary imbibition: A study on how compaction bands impact fluid flow in Bentheim sandstone. *Journal of Geophysical Research*, *116*, B03205. https://doi.org/10.1029/2010JB007973

Prasad, M., & Manghnani, M. H. (1997). Effects of pore and differential pressure on compressional wave velocity and quality factor in Berea and Michigan sandstones. *Geophysics*, *62*(4), 1163–1176. https://doi.org/10.1190/1.1444217

Prasad, M., & Meissner, R. (1992). Attenuation mechanisms in sands: Laboratory versus theoretical (Biot) data. *Geophysics*, *57*(5), 710–719. https://doi.org/10.1190/1.1443284

Sarout, J. (2012). Impact of pore space topology pn permeability, cut-off frequencies and validity of wave propagation theories. *Geophysical Journal International*, *189*(1), 481–492. https://doi.org/10.1111/j.1365-246X.2011.05329.x

Subramaniyan, S., Quintal, B., Madonna, C., & Saenger, E. H. (2015). Laboratory-based seismic attenuation in Fontainebleau sandstone: Evidence of squirt flow. *Journal of Geophysical Research: Solid Earth*, *120*, 7526–7535. https://doi.org/10.1002/2015JB012290

Tittmann, B. R. (1977). Lunar rock Q in 3000-5000 range achieved in laboratory. *Philosophical Transactions of the Royal Society of London. Series A, Mathematical and Physical Sciences*, *285*(1327), 475–479. https://doi.org/10.1098/rsta.1977.0090

Tittmann, B. R. (1978). Internal friction measurements and their implications in seismic Q structure models of the crust. *Geophysical Monograph Series*, *20*, 197–213.

Tittmann, B. R., Clark, V. A., Richardson, J. M., & Spencer, T. W. (1980). Possible mechanism for seismic attenuation in rocks containing small amounts of volatiles. *Journal of Geophysical Research*, *85*(B10), 5199–5208. https://doi.org/10.1029/JB085iB10p05199

Tittmann, B. R., Clark, V. A., & Spencer, T. W. (1980). Compressive strength, seismic Q, and elastic modulus. In *Lunar and Planetary Science Conference Proceedings* (Vol. 11, pp. 1815–1823). Woodlands, TX: Lunar and Planetary Institute.

Toksöz, M. N., Cheng, C. H., & Timur, A. (1976). Velocities of seismic waves in porous rocks. *Geophysics*, *41*(4), 621–645. https://doi.org/10.1190/1.1440639

Toksöz, M. N., Johnston, D. H., & Timur, A. (1979). Attenuation of seismic waves in dry and saturated rocks: I. Laboratory measurements. *Geophysics*, *44*(4), 681–690. https://doi.org/10.1190/1.1440969

Winkler, K. W., & Murphy, W. F. III (1995). Acoustic velocity and attenuation in porous rocks. In *Rock physics and phase relations, A handbook of physical constants*, *Refrence Shelf* (Vol. 3, pp. 20–34). Washington, DC: American Geophysical Union.

Yurikov, A., Lebedev, M., Gor, G. Y., & Gurevich, B. (2018). Sorption-induced deformation and elastic weakening of Bentheim sandstone. *Journal of Geophysical Research: Solid Earth*, *123*, 8589–8601. https://doi.org/10.1029/2018JB016003